Micro-seismic event estimation using an efficient wavefield inversion method

Chao Song and Tariq Alkhalifah, King Abdullah University of Science and Technology.

SUMMARY

Micro-seismic event estimation results depend highly on the velocity accuracy. Full waveform inversion (FWI) has been employed to invert for the velocity and micro-seismic source image, simultaneously. However, conventional FWI suffers from the infamous cycle-skipping problem, which is even more serious when the source location is unknown. To mitigate this issue, we formulate an optimization problem to linearly reconstruct the wavefield in an efficient matter using the background model information and allow an enhanced source function to absorb the secondary (perturbation) source information. This reconstructed wavefield is then used to update this enhanced source function using the same background wave equation modeling operator without any inversion or update process. We then use the reconstructed wavefield to extract from the enhanced source function the parts corresponding to the micro-seismic source image and those corresponding to secondary sources (velocity perturbations), which can be used to update the model. In the outer loop iterations we repeat the processes of inverting for the source and updating the model until we achieve convergence. This process and its effectiveness is demonstrated on a complicated synthetic model and a field dataset.

INTRODUCTION

Micro-seismic event estimation helps engineers monitor the subsurface processes and optimize injection strategies. Time-reversal propagate the recoded data backward to reconstruct the wavefield using the wave equation (Artman et al., 2010). With an appropriate imaging condition, a source image can be obtained (Nakata and Beroza, 2016; Rocha et al., 2018). This category of methods highly depend on the accuracy of the velocity model. Besides velocity information, the uncertainties of the source wavelet and source-origin time also make the wavefield reconstruction more difficult (Song et al., 2017). In order to solve these probelms, simultaneous inversion of the source function and velocity model is required. Full-waveform inversion (FWI) has been utilized to invert for the source compenents and the vleocity. Wang and Alkhalifah (2018) introduced a source-independent FWI method to invert for the velocity model and source components, simultaneously. Wu and Alkhalifah (2017) proposed a source-extension approach to determine the source location while inverting for the velocity and source image simultaneously in the frequency domain. To further improve this method, Song et al. (2019b) proposed to use multi-scattered energy in the data to provide better illumination to the velocity model. They use a penalty term in the misfit function to enforce a focused source image. This penalty function used to measure the source image focusing property is applied as an objective function to optimized the source image and velocity model, simultaneously (Song et al., 2019a). Conventional FWI is based on minimizing the difference between the calculated and the recorded data in a least-square sense subject to the wave equation. We use a modification to the wavefield reconstruction inversion (WRI) method (Leeuwen and Herrmann, 2013), we refer to as efficient wavefield inversion (EWI), to invert for the source function and velocity model, simultaneously. As the wavefield in the model space can be reconstructed using the augmented wave equation, the unknown micro-seismic source function can be easily calculated without any inversion process. The velocity perturbation can be calculated via direct division (Alkhalifah and Song, 2019).

In this abstract, we use EWI to invert for the source function and velocity model, simultaneously. As the wavefield in the model space can be reconstructed using the augmented wave equation, the unknown micro-seismic source function can be easily calculated without any inversion process. The velocity perturbation can be calculated via direct division. Application on a modified Marmousi model shows that the proposed approach can yield a reasonably good inverted velocity model, which can help locate micro-seismic events accurately. We demonstrate the effectiveness of the proposed method with a field dataset.

THEORY

In the conventional FWI implementation, we tend to measure the misfit between the recorded and calculated data from a wavefield that satisfies the wave equation, which can be expressed in short form as:

$$J(V,f) = min\frac{1}{2}\|d - Cu\|_2^2 \quad s.t. \quad L(V,\omega)u = f(\mathbf{x},\omega), \quad (1)$$

where, d is the recorded data, and C is the mapping operator, which projects the wavefield to the receiver positions. We use u to represent the wavefield, and $L(V) = \nabla^2 + (V_0 + V)\omega^2 = L_0 + \omega^2 V$ is the modelling operator, with the operator $L_0(V_0) = \nabla^2 + V_0\omega^2$ corresponding to the background squared slowness V_0. We use V as the squared slowness perturbation, and set it to zero at the beginning of the inversion process. As we implement this method in the frequency domain, the source origin time uncertainty is mitigated. The source function $f(\mathbf{x},\omega)$ made up of complex values includes both wavelet and spatial information. The amplitude of $f(x,\omega)$ represents the spatial feature of the source function, which is referenced as the source image $[f(\mathbf{x},\omega)]$. Based on the adjoint-state method, the source function gradient is given by:

$$\nabla_f J = \sum_{\omega} \omega^2 L^{-1}(C^T \Delta d) \quad (2)$$

where $\Delta d = d - Cu$ is data residual, $L^{-1}(C^T \Delta d)$ is the back-propagated wavefield. The high non-linearity in the conventional FWI has always been a big challenge. In order to solve

this problem, the objective function of EWI is given by Alkhalifah (2018):

$$E(u, f_e) = min \frac{1}{2} \|d - Cu\|_2^2 + \frac{\varepsilon}{2} \|L_0 u - f_e\|_2^2 . \quad (3)$$

In equation 3, f_e is a modified source function, which contains, in addition to the true source function, the secondary sources (perturbations). We derive this modified source by splitting the velocity model into the background squared slowness and the squared slowness perturbation.

$$Lu = f \rightarrow (L_0 + \omega^2 V)u = f \rightarrow f_e = f - \omega^2 V u \quad (4)$$

The wavefield at each frequency satisfies the following linear equation:

$$\begin{pmatrix} \varepsilon L_0 \\ C \end{pmatrix} u = \begin{pmatrix} \varepsilon f_e \\ d \end{pmatrix}. \quad (5)$$

In the micro-seismic case, the source function is unknown. We initialize the inversion with $f_{e0} = 0$. After obtaining the wavefield u using equation 5, the source function can be calculated by

$$f_{e0}(\mathbf{x}) = \sum_{\omega} L_0(\omega) u(\omega). \quad (6)$$

In equation 6, the inverted source function $f_{e0}(\mathbf{x})$ is obtained by stacking over all frequencies. This will provide a source image focused mainly on the original source, especially since the direct arrivals are often the strongest, but it will include some weaker secondary sources courtesy of the perturbations. We use a source optimization function to focus the source energy more focused in the source image. The source optimization function is (Wang et al., 2018):

$$J(f_{op}, \mathbf{x_s}) = \frac{1}{2} \sum_{\mathbf{x}} \left\| f_{op}(\mathbf{x}) - f_0(\mathbf{x}) \right\|_2^2 + \frac{\alpha}{2} \sum_{\mathbf{x}} \|(\mathbf{x} - \mathbf{x_s}) f_0(\mathbf{x})\|_2^2 , \quad (7)$$

where $f_0(\mathbf{x})$ is the input source function, and $f_{op}(\mathbf{x})$ is the output optimized source function. $\mathbf{x_s}$ denotes the estimated source location coordinate, and α is the weighting parameter controlling the focusing amount of the source function. The basic idea of equation 7 is to penalize non-physical source energy away from $\mathbf{x} = \mathbf{x_s}$ in the source function. We set $\frac{\partial J}{\partial \mathbf{x_s}} = 0$ and $\frac{\partial J}{\partial f_{op}} = 0$ to calculate the estimated source location coordinate $\mathbf{x_s}$:

$$\mathbf{x_s} = \frac{\sum_{\mathbf{x}} f_0(\mathbf{x})^2 \mathbf{x}}{\sum_{\mathbf{x}} f_0(\mathbf{x})^2} \quad (8)$$

where

$$f_{op}(\mathbf{x}) = \frac{f_0(\mathbf{x})}{1 + \alpha(\mathbf{x} - \mathbf{x_s})^2}. \quad (9)$$

We can use the inverted source function $f_{e0}(\mathbf{x})$ (or optimized one $f_{op}(\mathbf{x})$) to calculate the wavefield $\hat{u}$ using equation 5. This source optimization function is only applicable for single event scenario, and it works well with the field data as we will see later. The modified source function f_e including the squared slowness perturbation can be calculated using the wave equation: $f_e = L_0 \hat{u}$. Following the relationship between the modified and original source function in equation 4, we approximately update the squared slowness using:

$$V \approx \frac{(f_{e0} - f_e)\hat{u}^*}{\omega^2 \hat{u}\hat{u}^* + \lambda}, \quad (10)$$

where λ is a small value to avoid dividing over zero. We update the background squared slowness model as: $V_0 = V_0 + V$. In each selected frequency, we calculate the squared slowness perturbation and update the background operator L_0 for the next frequency. The frequency domain FWI and WRI use considerable number of iterations in each frequency to update the model. By comparison, EWI is capable of calculating the squared slowness perturbation directly. To summarize our approach, we first need to invert for the source function. Then we use it as the source function to calculate the squared slowness perturbation and update the background operator. We need to use outer loops to repeat these two nested steps until convergence is achieved.

EXAMPLES

We first consider a homogeneous model of size 200×200 samples. The true source location is in the middle of the model. All the grid points on the surface act as receivers given by the $\triangle$ symbol shown in Figure 1a. We perform the source function inversion starting from 3 Hz to 8 Hz with a frequency interval of 0.5 Hz. The true and inverted wavefields obtained from equation 3 for 8 Hz is shown in Figure 1b. We initialize the modified source f_e to zero. As data are only recorded on the surface, the wavefield near the surface is well reconstructed. The inverted source image is shown in Figure 2a, and the optimized source image is shown in Figure 2b. We see that the source energy in the original inverted source image is well focused on the true source location. However, there are some artifacts around the source location. After optimizing the original inverted source image using equation 9, the source energy is better focused and the artifacts are suppressed. However, this is only applicable in the single event case.

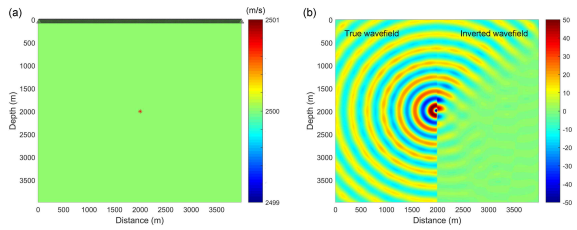

Figure 1: Homogeneous velocity model with receivers on the surface ($*$ denotes the true source location).

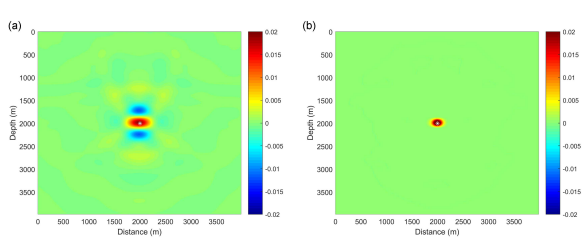

Figure 2: The original inverted source image (a) and optimized source image (b) using the true velocity ($*$ denotes the true source location).

We apply the proposed method including the velocity inversion on a modified Marmousi model of size 370×80 samples. The true velocity model is shown as in Figure 3. We use two sources igniting simultaneously, and are located at (3700 m, 1000 m) and (3700 m, 1400 m), as the red star $*$ symbols indicate. We use a linearly increasing with depth model as the initial model, which is shown in Figure 4a. The inverted source image corresponding to the initial velocity model is shown in Figure 4b. We observe that the source energy is not focused at the true source locations due to the error in the velocity model. To improve the source image quality, we use 30 iterations to perform the simultaneous inversion of the source image and the velocity model. The inverted velocity model and the final source image are shown in Figures 5a and 5b, respectively. As the inversion is dominated by transmissions, the kinematic features of the Marmousi model is reasonably recovered in the inverted model. As a result, the source energy in the final source image is focused very close to the true source locations. The slight difference is due to the approximation we made to have the inverted source image in the first iteration to be the true source image, which implies we are focusing direct arrivals in the inversion. To demonstrate the superiority of the proposed method, we implement FWI to invert for the source image and velocity with the same inversion setup (Song et al., 2019b). The inverted velocity and source image using FWI are shown in Figures 6a and 6b. From Figure 6b, it is obvious that the source image using FWI has lower resolution than that from EWI. The source energy is not fully focused to the true source location.

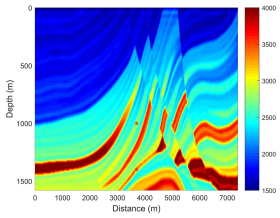

Figure 3: The true modified Marmousi model with two sources ($*$ denotes the true source location).

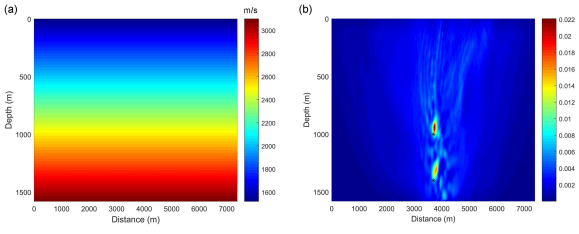

Figure 4: The true modified Marmousi model with two sources ($*$ denotes the true source location) using EWI.

We further test our proposed method on a single micro-seismic event captured in the field. This field dataset is collected from an oil field in China during an 11-stage hydraulic fracturing treatment. The recording system used in this survey consists of 15 levels of three-component geophones. The geometry, which includes a treatment well (blue dots), a monitoring well

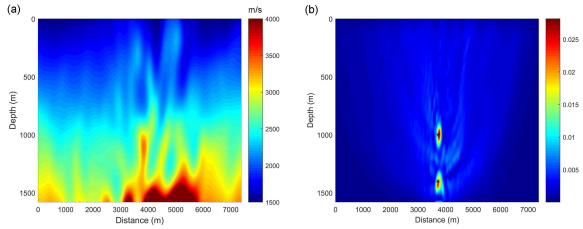

Figure 5: The true modified Marmousi model with two sources ($*$ denotes the true source location) using EWI.

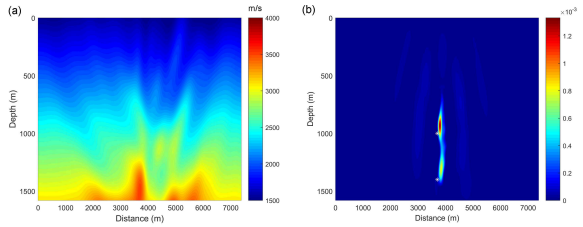

Figure 6: The true modified Marmousi model with two sources ($*$ denotes the true source location) using FWI.

(red dots) and receivers (black triangles) shown in Figure 7. We focused on the single event in Figure 8, and muted all the arrivals afterwards. We first choose one trace of the recorded data and analyse the frequency spectrum. The trace and its frequency spectrum are shown in Figures 9a and 9b, respectively. We conduct a bandpass filter between 10 Hz and 30 Hz. The filtered data spectrum and the corresponding data are shown in Figures 9c and 9d, respectively. We use a homogeneous velocity model of 4000 m/s as the initial velocity, which is shown in Figure 10a.

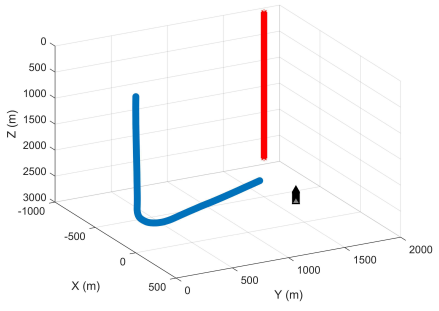

Figure 7: Field data collecting geometry with treatment well (blue dots), monitoring well (red dots) and receiver (black triangles).

As low-frequency components in the data are missing, we conduct the inversion process process from 10 Hz to 30 Hz with a sampling interval of 0.15 Hz. In each selected frequency, we use two inner iterations. The source image corresponding to the initial velocity model is shown in Figure 10b. As the initial velocity is very bad, the corresponding source image has a poor focusing feature, even though we use the optimized source function with $\alpha = 0.001$. After 25 iterations of veloc-

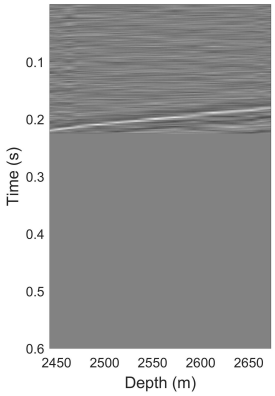

Figure 8: The original data.

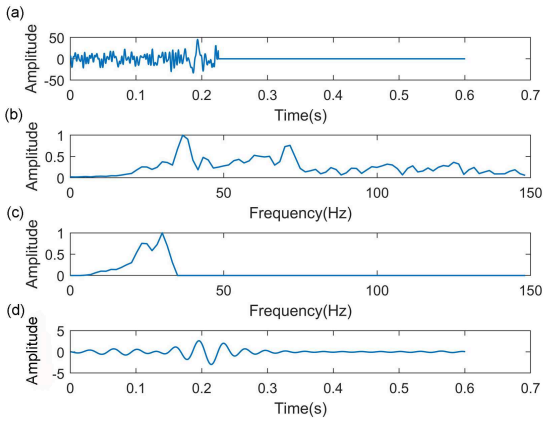

Figure 9: One trace of the data (a), the frequency spectrum of this trace (b), the frequency spectrum after bandpass (c), and the trace after bandpass filtering.

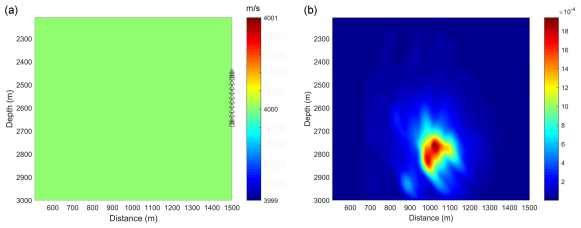

Figure 10: The initial homogeneous velocity model (a) and the inverted source image with the initial velocity (b).

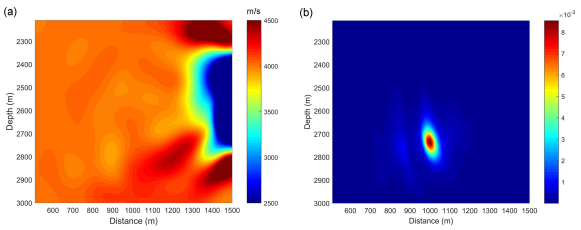

Figure 11: The inverted velocity model (a), and the final inverted source image (b).

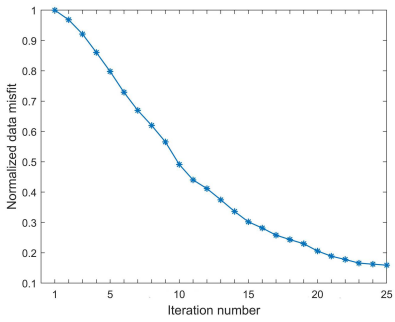

Figure 12: The misfit decreasing curve of the 25 iterations.

ity update corresponding to the number of frequency bands, the inverted velocity is shown in Figure 11a. It is obvious that there is a low velocity zone in the survey area. It is reasonable as the low velocity zone corresponds to the fluid injection well location. The inverted source image obtained from the inverted velocity model is shown in Figure 11b, and the source energy is focused better with the same α in the source optimization. From the normalized data misfit curve shown in Figure 12, the inversion process is converging.

CONCLUSIONS

We introduced a new micro-seismic event estimation method based on EWI. This new method is reasonably immune to the cycle-skipping problem, as well as a bad initial guess of source location often impeding FWI implementations. It also mitigates uncertainties of the source wavelet and origin time in micro-seismic event estimation. We use the augmented wave equation to reconstruct the wavefield and calculate the source function. We apply a source optimization problem to get a focused source image. Then we proposed to use the EWI method to optimize the velocity model in an efficient way. Applications to data generated from a modified Marmousi with simultaneous multiple sources yield reasonably good results. The application on field data also shows that the proposed method can get reasonable velocity inversion results and the improve source image quality.

ACKNOWLEDGMENTS

We thank KAUST for its support and the SWAG group for the collaborative environment. This work utilized the resources of the Supercomputing Laboratory at King Abdullah University of Science and Technology (KAUST) in Thuwal, Saudi Arabia, and we are grateful for that.

REFERENCES

Alkhalifah, T., 2018, Linear wavefield optimization using a modified source: Communications in computational physics, accepted.

Alkhalifah, T., and C. Song, 2019, An efficient wavefield inversion: 81th EAGE Conference and Exhibition 2019.

Artman, B., I. Podladtchikov, and B. Witten, 2010, Source location using time-reverse imaging: Geophysical Prospecting, **58**, 861–873.

Leeuwen, T. V., and F. Herrmann, 2013, Mitigating local minima in full-waveform inversion by expanding the search space: Geophysical Journal International, **195**, 661–667.

Nakata, N., and G. C. Beroza, 2016, Reverse time migration for microseismic sources using the geometric mean as an imaging condition: Geophysics, **81**, 51–60.

Rocha, D., P. Sava, J. Shragge, and B. Witten, 2018, 3d passive wavefield imaging using the energy norm: Geophysics, **84**, 1–98.

Song, C., T. Alkhalifah, and Z. Wu, 2019a, Micro-seismic event estimation and velocity analysis based on a source-focusing function: Geophysics, **84**, 1–42.

Song, C., T. Alkhalifah, Z. Wu, and B. Sun, 2017, Non-stationary filter used in micro-seismic source imaging: 87th Annual International Meeting, SEG, Expanded Abstracts, 2898–2902.

Song, C., Z. Wu, and T. Alkhalifah, 2019b, Passive seismic event estimation using multi-scattering waveform inversion: Geophysics, **84**, 1–38.

Wang, H., and T. Alkhalifah, 2018, Microseismic imaging using a source function independent full waveform inversion method: Geophysical Journal International, **214**, 46–57.

Wang, H., Q. Guo, T. Alkhalifah, and Z. Wu, 2018, Regularized passive elastic full-waveform inversion with an unknown source: SEG Technical Program Expanded Abstracts 2018, 2932–2936.

Wu, Z., and T. Alkhalifah, 2017, A new wave equation based source location method with full-waveform inversion: 74th Annual International Conference and Exhibition, EAGE, Extend Abstracts, Th P6 15.